TAUP XICHANG

The Event Discrimination in the Bulk Region of Point-Contact Germanium Detector

Li Renmingjie

Sichuan University

CDEX CJPL

Motivation

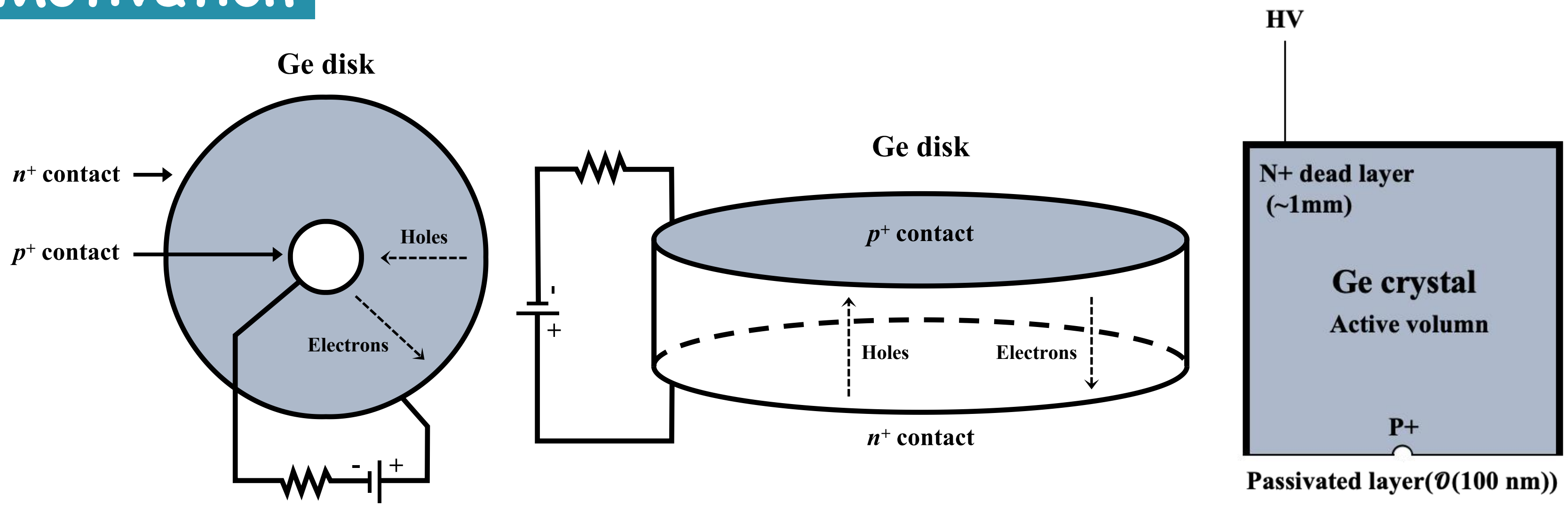

Fig.1 Schematic diagram of high-purity germanium detector

Characteristics:

① Ultralow noise

② Low energy thresholds

③ Excellent energy resolution

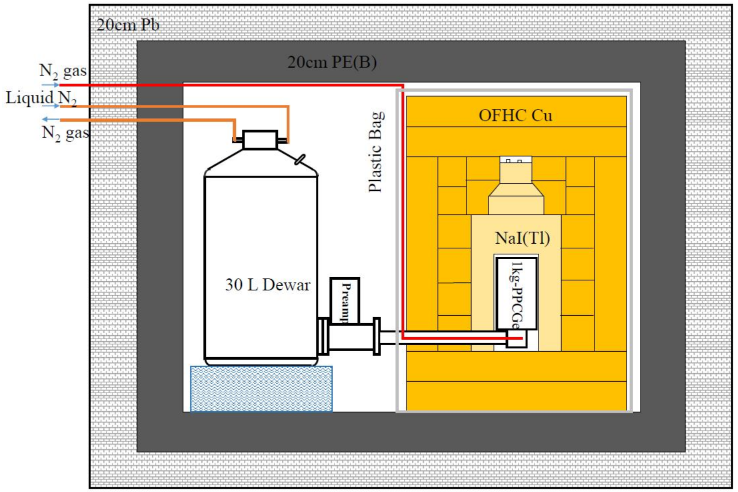

Fig.2 CDEX-1 system (*p*-type point-contact Ge detector, PPCGe)

Fig.3 The China Dark Matter Experiment (**CDEX**)

CDEX pursues:

⊙ Light dark matter

⊙ 0νββ-decay

With the goal of building

a ton-scale germanium detector array

at the CJPL

Motivation

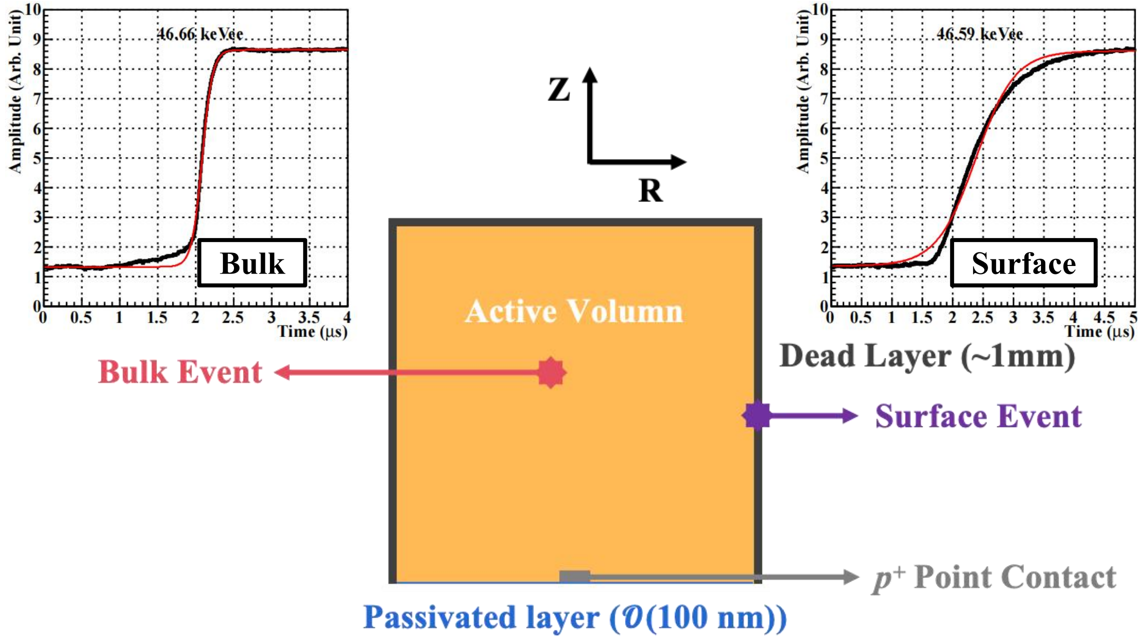

Fig.4 Schematic diagram of a typical *p*PCGe detector

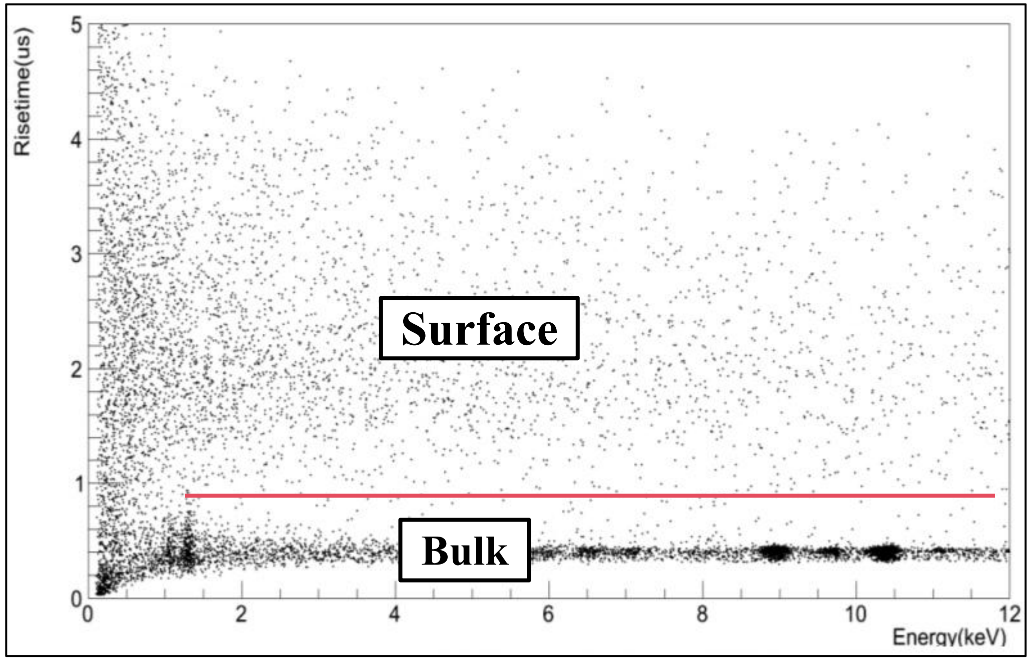

C1B

Fig.5 Scatter plots of rise-time[1] versus energy in low-energy regions, from CDEX-1B detector data

Two types of events were observed:

① Surface events(SEs) deposit energy in the dead layer

② Bulk events(BEs) deposit energy in the detector's active volume

Pulse shape feature:

SEs
- ⊙ Incomplete charge collection
- ⊙ Slow rising pulse

BEs
- ⊙ Complete charge collection
- ⊙ Relatively fast rising pulse → **Fig.5**

[1]Define **rise-time** parameter (the time interval between 5% and 95% of the pulse amplitude) to quantify this rising characteristic

Motivation

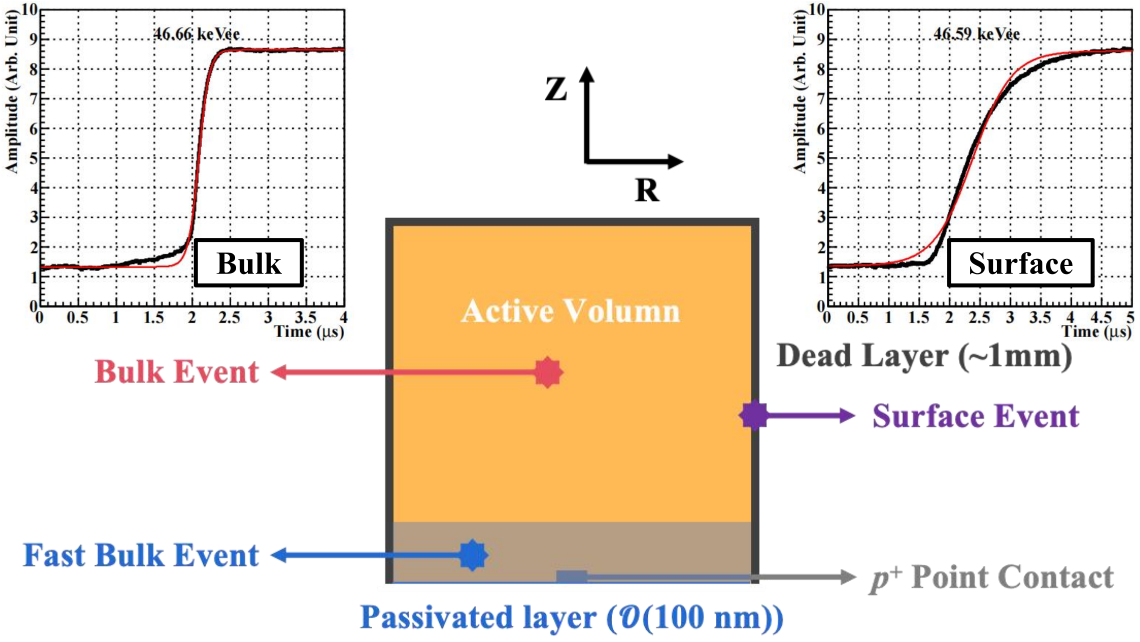

Fig.4 Schematic diagram of a typical *p*PCGe detector

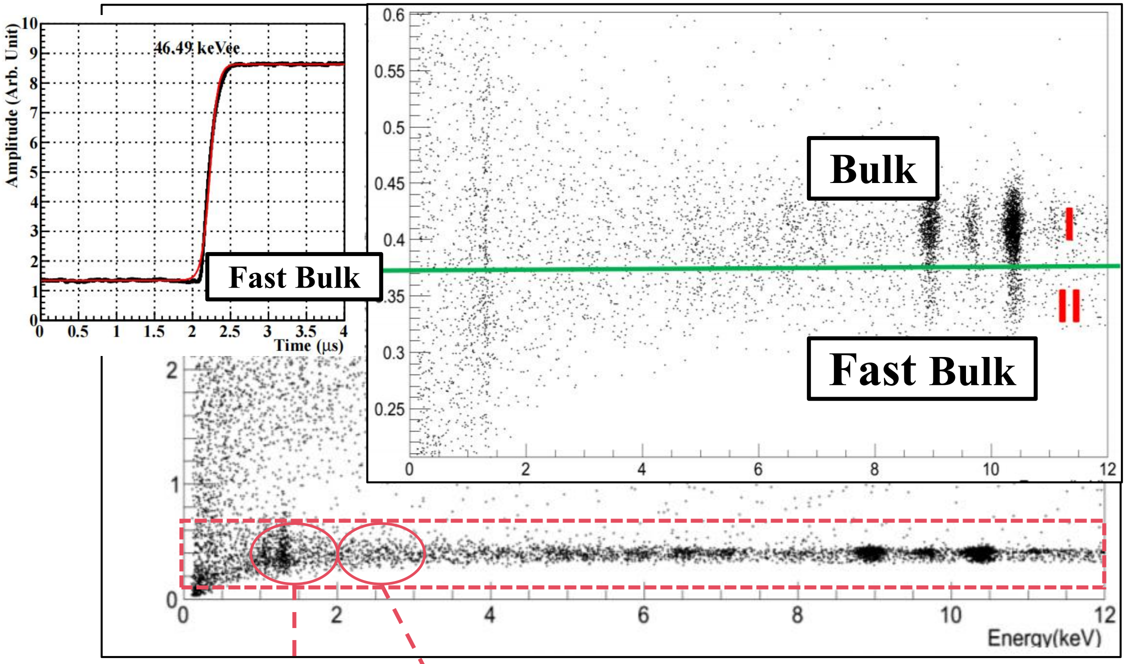

Fig.5 Scatter plots of rise-time[1] versus energy in low-energy regions, from CDEX-1B detector data

▎Abnormal events:

The bulk distribution, exhibits an abnormal structure: some events show an extremely fast rising pulse compared to typical BEs. (Fast Bulk Events, FBEs)

▎Cross-contamination in low energy region:

① BEs and FBEs can be roughly distinguished above 10 keVee

② and exhibit serious cross-contamination below 5 keVee.

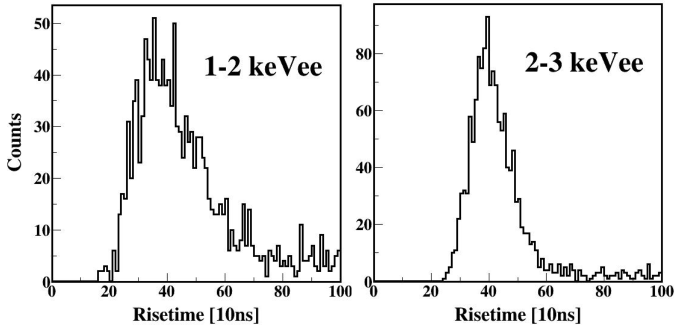

Motivation

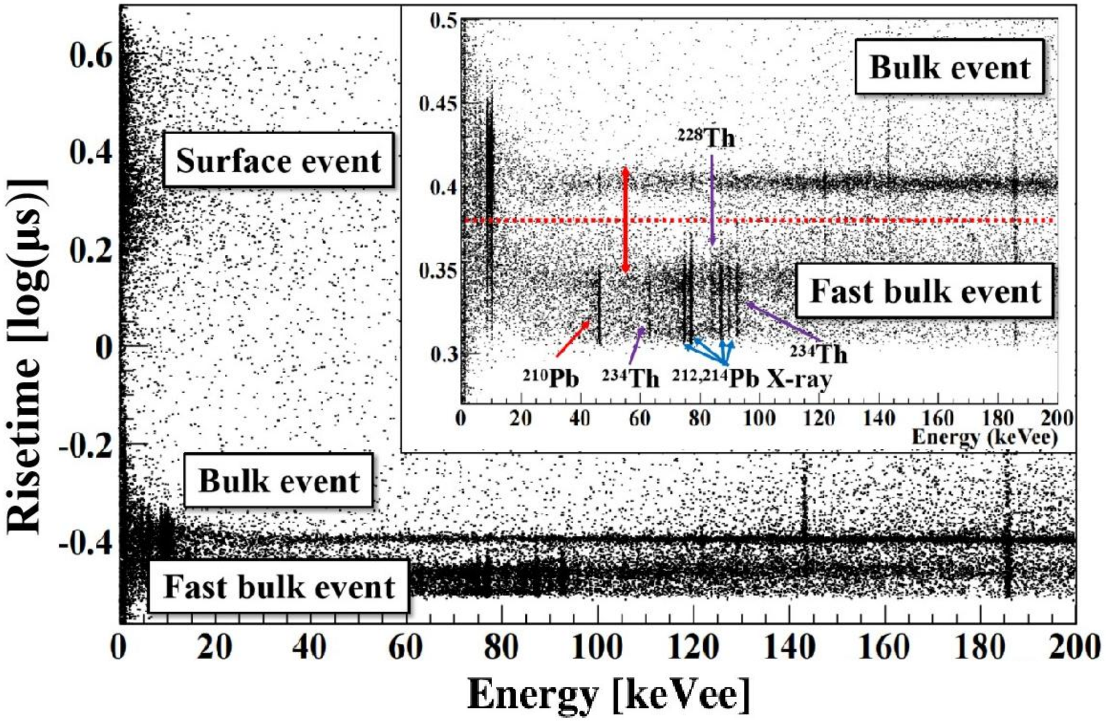

Fig.6 Scatter plots of rise-time versus energy below 20 keVee

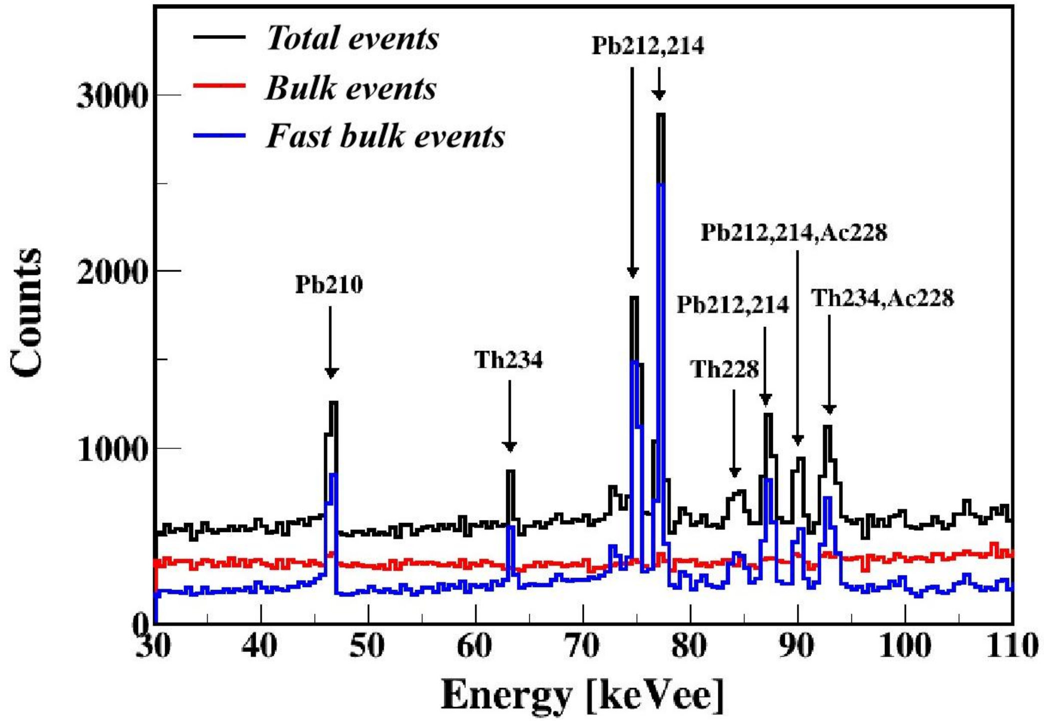

Fig.7 Background energy spectrum including BEs and FBEs in 30–110 keVee regions

Why do we focus on FBEs:

In the CDEX-1B background, for all the peaks below 100 keVee, most of the events correspond to FBEs.

These peaks are generated by γ rays or X-rays emitted by the progeny of ^{238}U and ^{232}Th.

Importance:

Removing FBEs will significantly reduce the CDEX background, thereby improving the sensitivity of dark matter searches.

Shockley-Ramo theorem:

For a deposited charge q ($q > 0$), the time-dependent induced signal $S(t)$ in the p$^+$ contact is given by:

$$S(t) = q\,[\boldsymbol{WP}(\boldsymbol{r}_h(t)) - \boldsymbol{WP}(\boldsymbol{r}_e(t))],$$ where $\boldsymbol{WP}(\boldsymbol{r}(t))$ represent the weighting potential at the position $\boldsymbol{r}(t)$. (h: hole, e:electron)

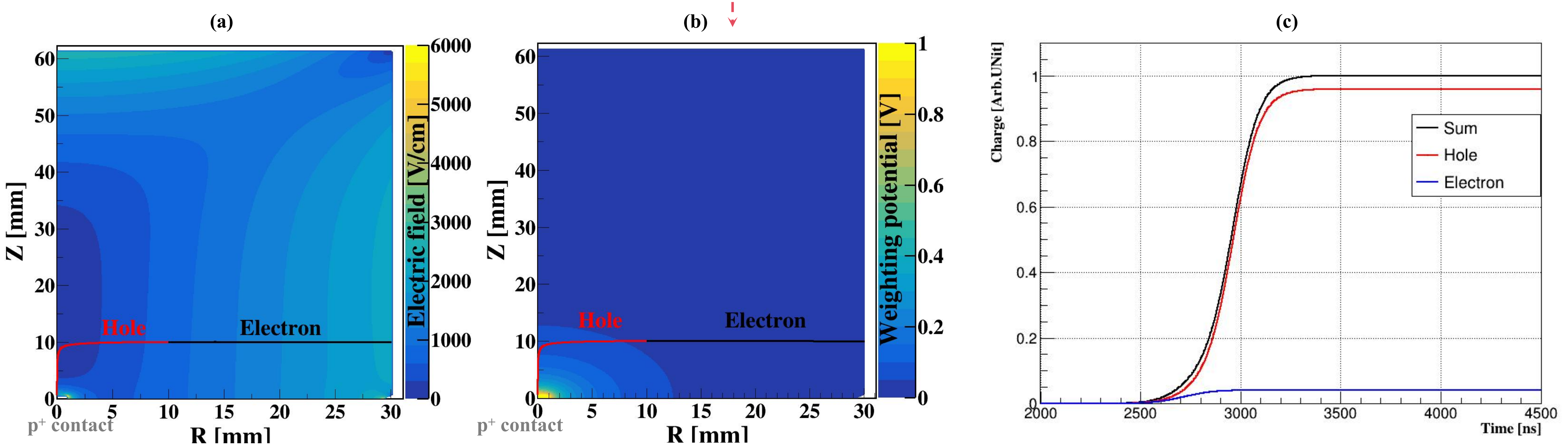

Fig.8 Simulated **(a)** electric field; **(b)** weighting potential; and **(c)** pulse shape with electronic response of the CDEX-1B detector, by the siggen software

Formation of FBEs pulse shape

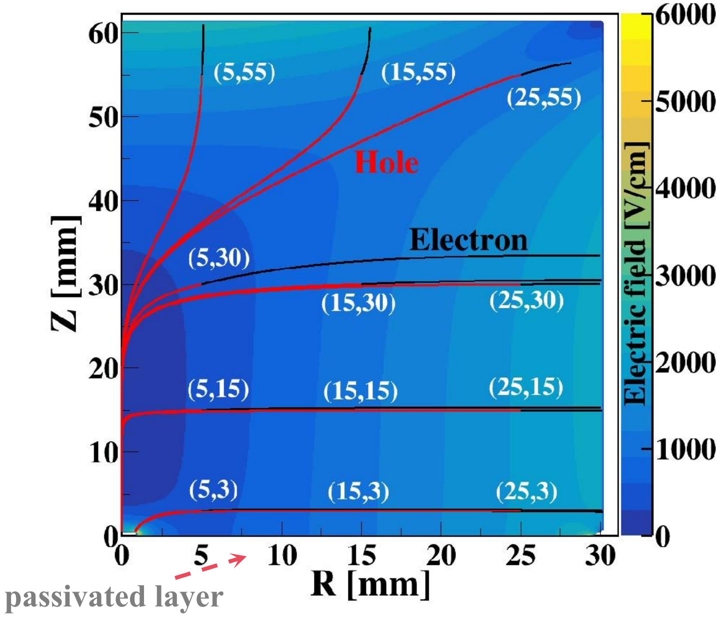

Fig.9 Drift paths of an electron-hole pair at different locations inside the detector

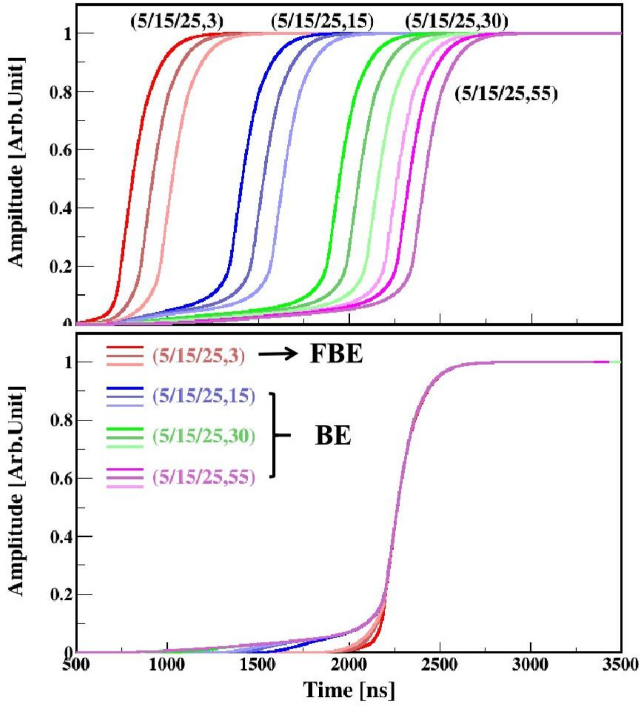

Fig.10 Corresponding induced signals. In the bottom panel, the points corresponding to half of the amplitude value of each signal are aligned

The origin of FBEs

- The hole carriers generated in most areas of the detector must pass through the weak field region, resulting in a longer rise time.
- The simulation confirms FBEs originate near the passivated layer, which is consistent with the analysis of the background spectrum reported above.

Experimental demonstration & Simulation comparison

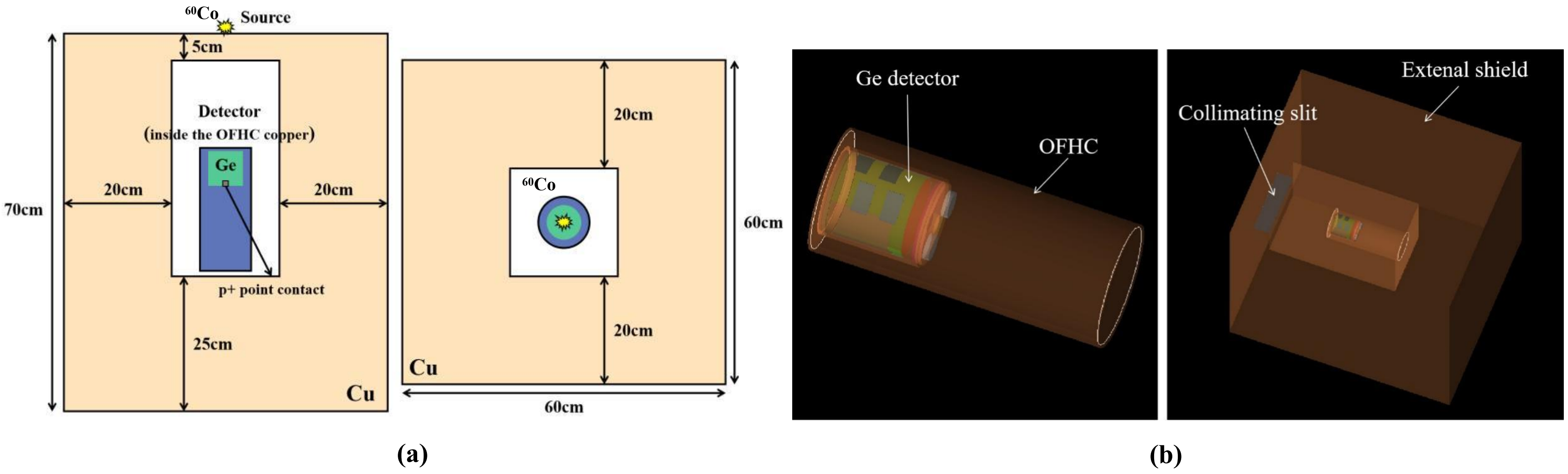

Fig.11 Schematic diagram of C1B detector and shielding from **(a)** experiment and **(b)** simulation for researching BEs and FBEs

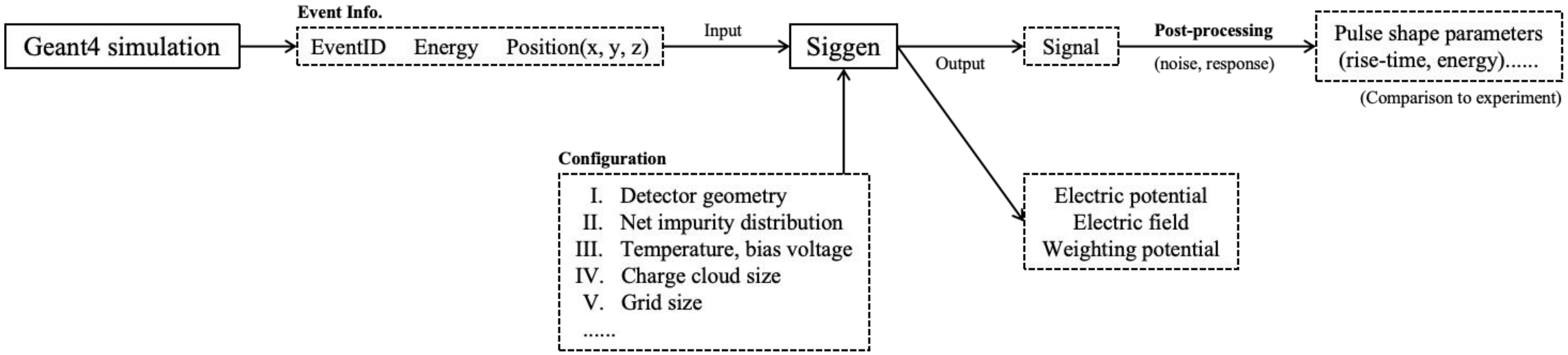

Fig.12 Flow-process diagram of pulse shape simulation

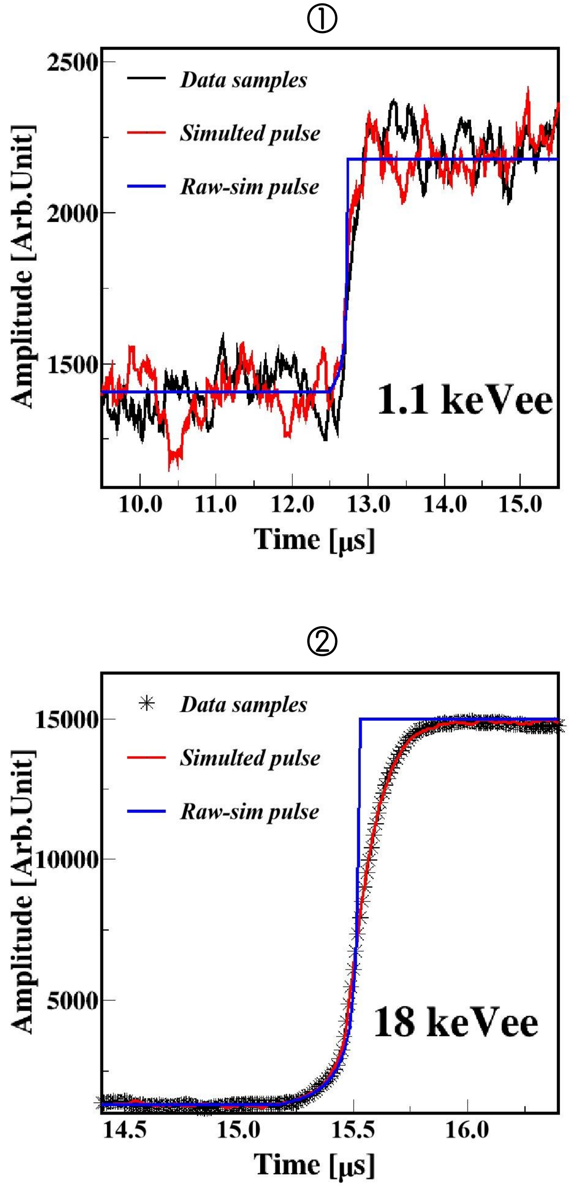

Fig.13 Raw pulses [blue] and post-processing pulse [red] at ①1.1 keVee and ②18 keVee

Experimental demonstration & Simulation comparison

[2]Here we only consider the events deposited in active volunm of detector. SEs have been cut.

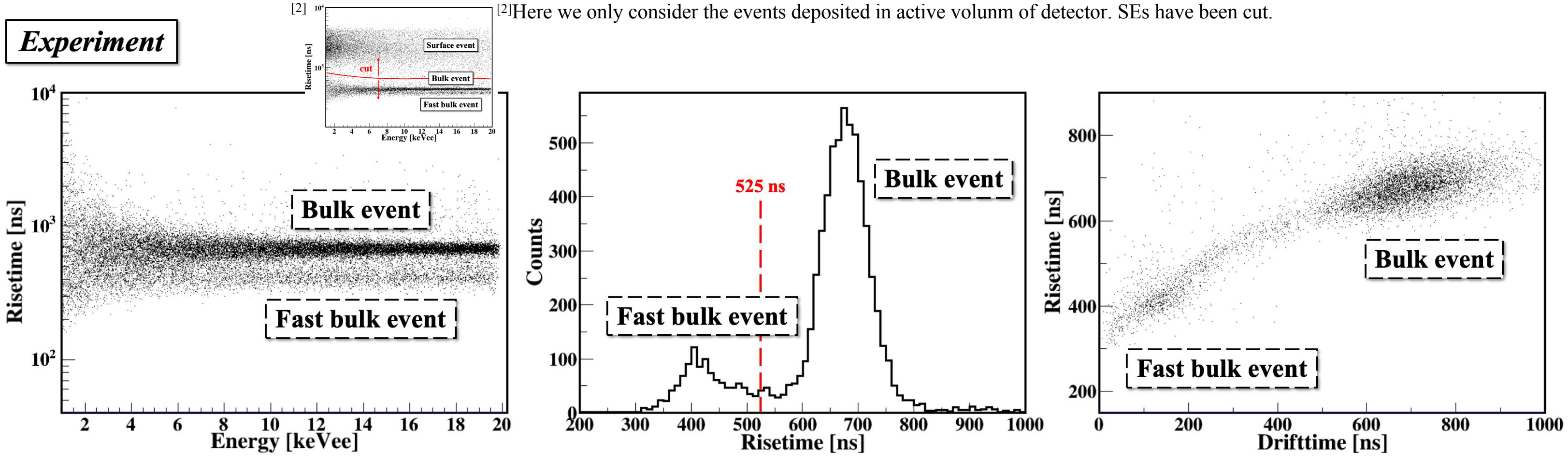

[3]the time interval between 1% and 5% of the pulse amplitude

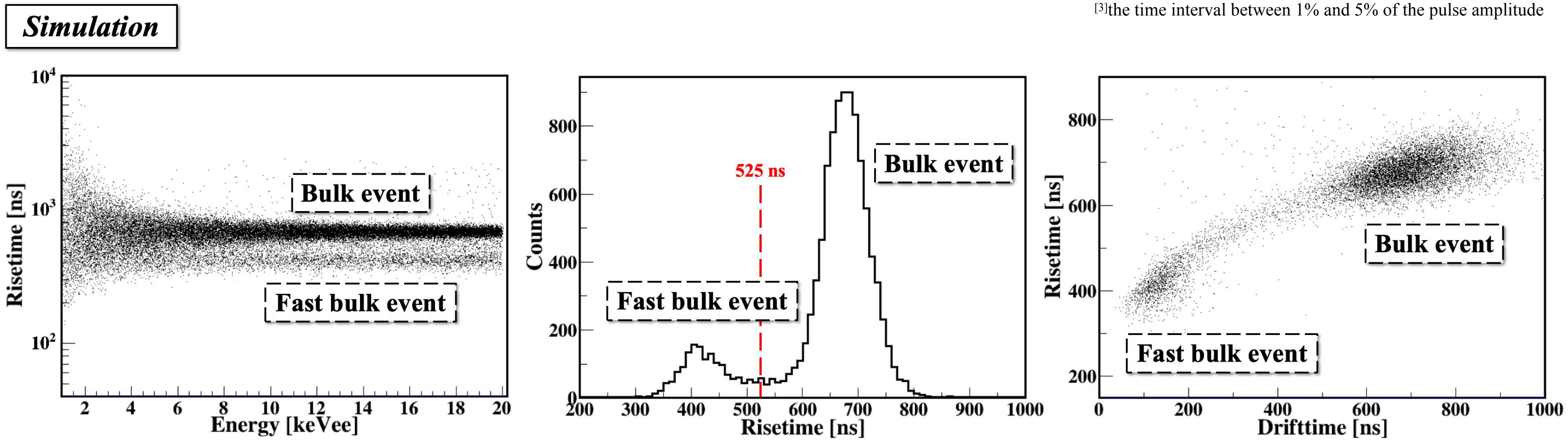

Fig.14 **(a)** Scatter plots of rise-time versus energy

(b) Rise time distributions of events with energy above 15 keVee

(c) Scatter plot of rise-time versus drift-time[3] for events with energies above 15 keVee

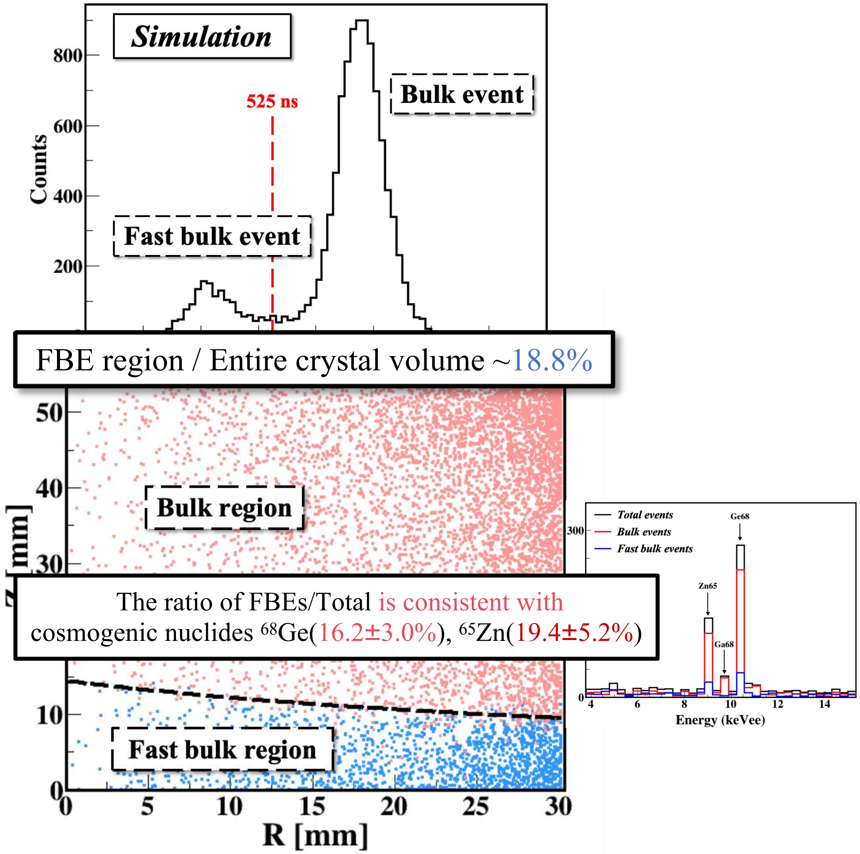

Fig.15 Simulated locations of FBEs and BEs in C1B detector obtained by simulations according to the 525 ns cut above 15 keVee

- **Good agreement:** The simulation are in good agreement with experiment
- **Consistency:** The volume ratio of the FBE region to the entire crystal is ~18.8 %, which is consistent with that derived from the ^{68}Ge peak and ^{65}Zn peak
- **Cross-contamination** can be observed in the ultra low energy regions, which causes the bands to merge

focus

BE and FBE discrimination

Rise-time PDFs:

Probability density functions (PDFs) of the rise-time distributions for BEs and FBEs can be obtained for different energy bins from simulations

Events discrimination:

Using two such PDFs to fit the rise-time distribution from the experiment

$$f_{BE}(E,\tau),\ f_{FBE}(E,\tau) \xrightarrow{\text{fit}^{[5]}} N_{Data}(E,\tau) \xrightarrow{\text{get}} N_{BE}(E,\tau),\ N_{FBE}(E,\tau)$$

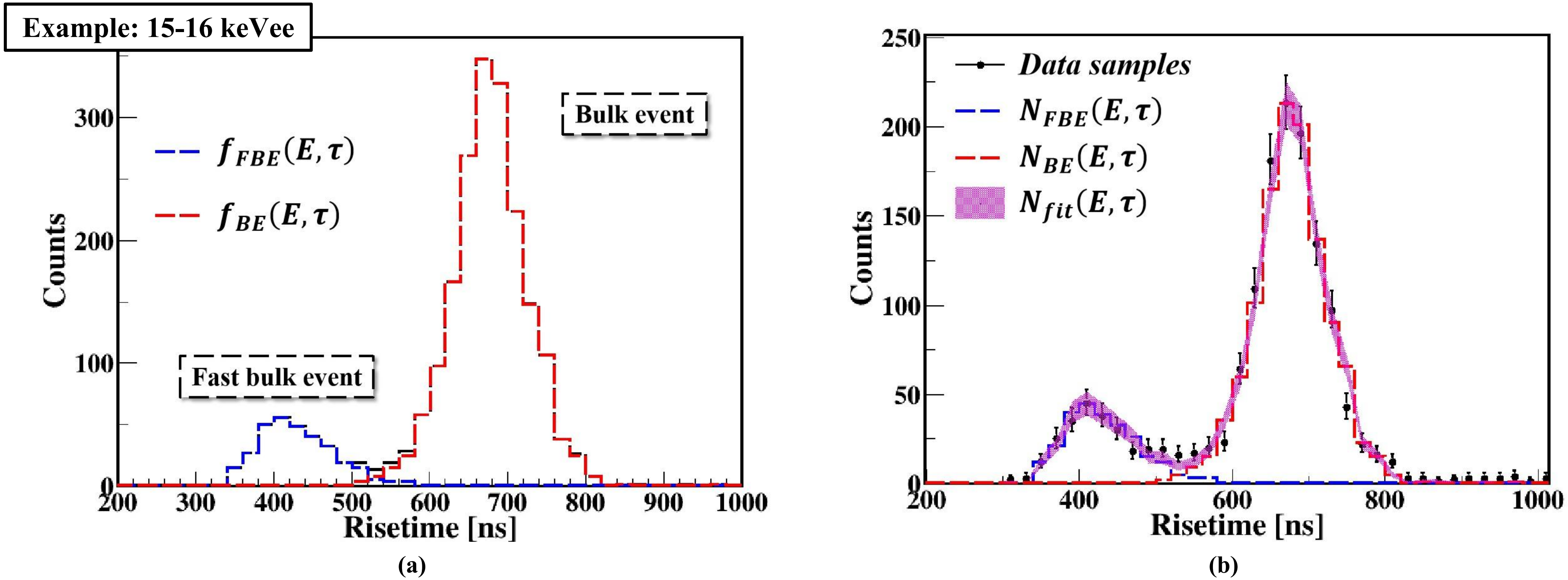

Fig.18 **(a)** The PDFs of BEs and FBEs obtained by simulations are used to **(b)** fit the experimental data

[5]An additional unitary constraint: (in the fitting interval) $Counts_{N_{fit}} = Counts_{data}$

BE and FBE discrimination

Good agreement:

All the fitting results for BEs and FBEs in different energy bins are in good agreement with the experiment

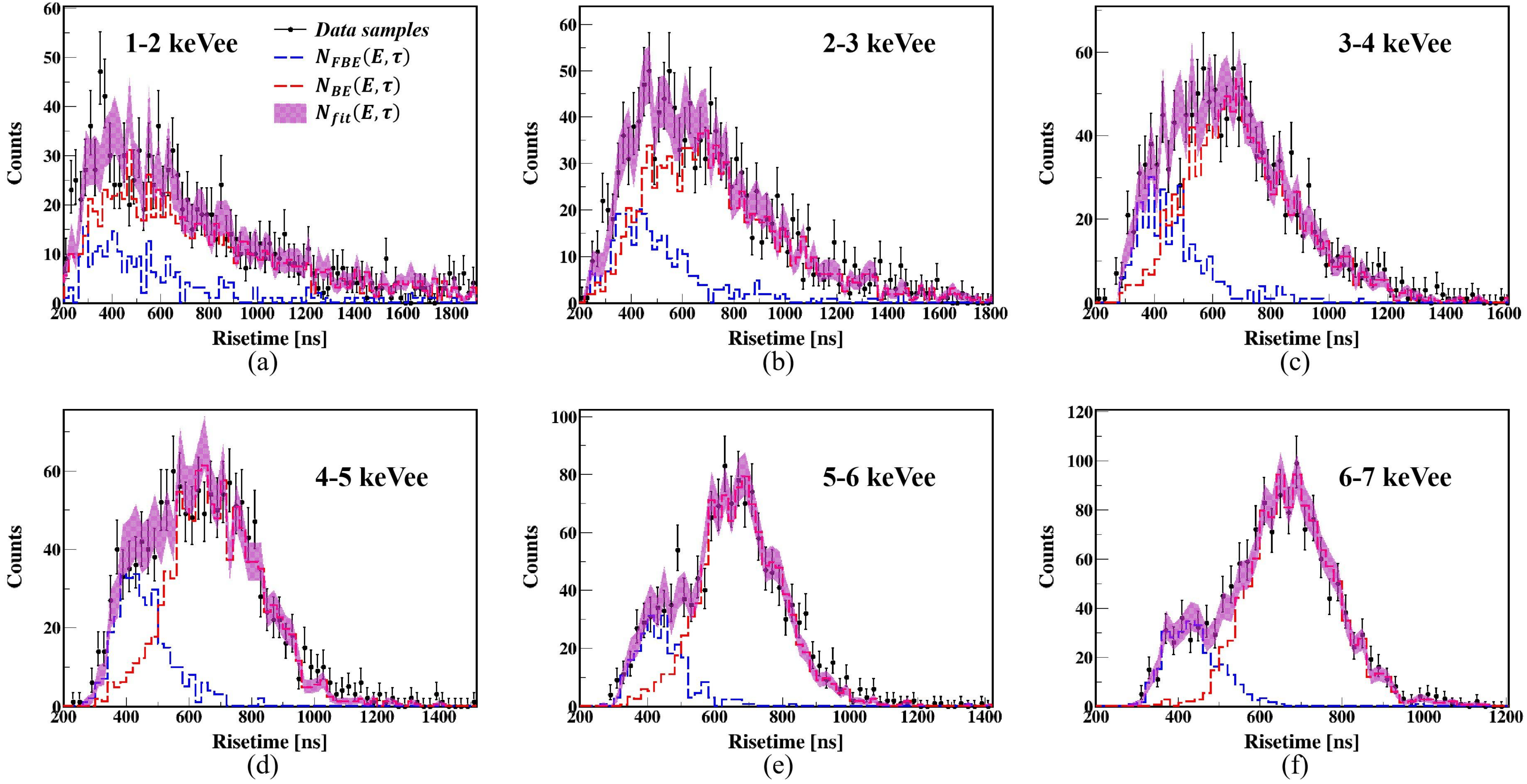

Fig.19 Fitting results in different energy ranges. **(a)** 1–2 keVee; **(b)** 2–3 keVee; **(c)** 3–4 keVee; **(d)** 4–5 keVee; **(e)** 5–6 keVee; **(f)** 6–7 keVee.

BE and FBE discrimination

$$C_{BE}(E) = \int_{all\,\tau} N_{BE}(E,\tau)\,d\tau$$
$$C_{FBE}(E) = \int_{all\,\tau} N_{FBE}(E,\tau)\,d\tau$$

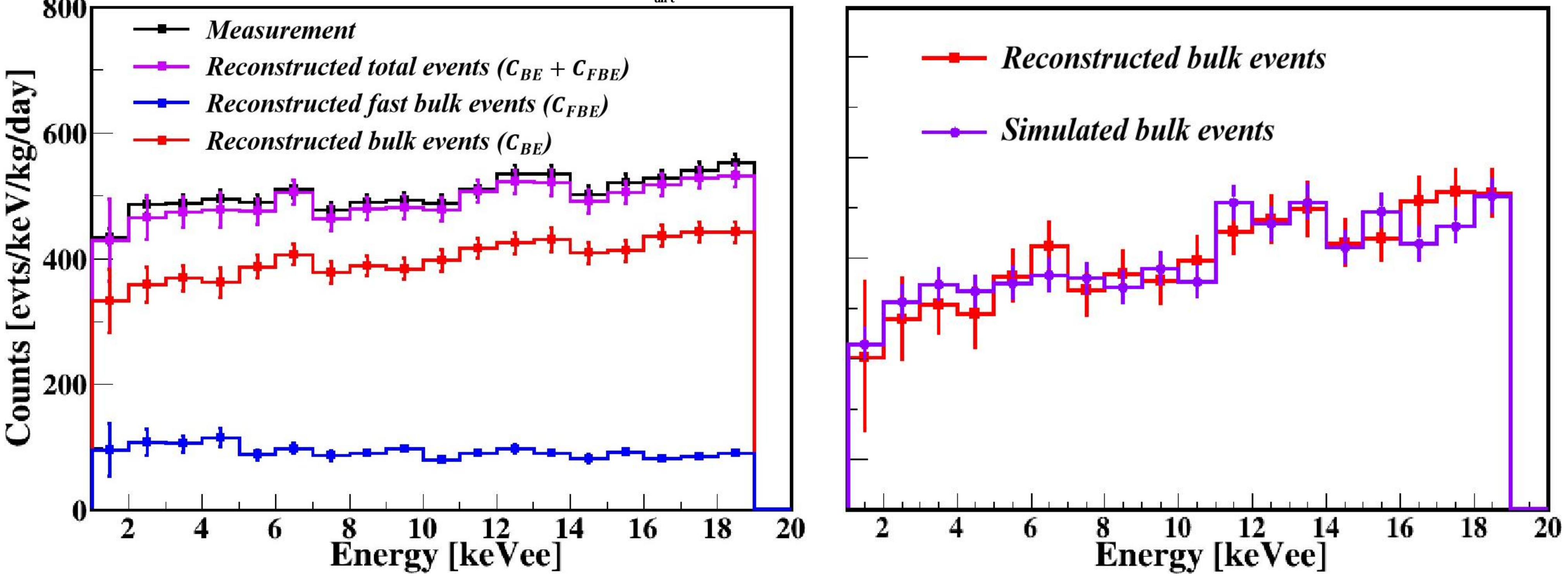

Fig.20 (a) Reconstructed energy spectrum (magenta), which contains BEs (red) and FBEs (blue), compared with experiment (black)

(b) Comparison of reconstructed bulk spectrum and G4 simulated bulk spectrum.

① The energy spectra for BEs and FBEs above 1 keVee are reconstructed — Significant impact of noise below 1keVee

② The reconstructed spectrum and simulated spectrum for BEs show a consistent trend — Credible

③ Removing FBEs can significantly reduce the event rate — Reduce the CDEX bacground

BE and FBE discrimination

Ultimate aim: To discriminate between FBEs and BEs in the background

- Various unknown and complex sources: how to determine the PDFs of BEs and FBEs from different type and position of sources?
- Analysis of background (preliminary work)
- Event discrimination below 1keVee?

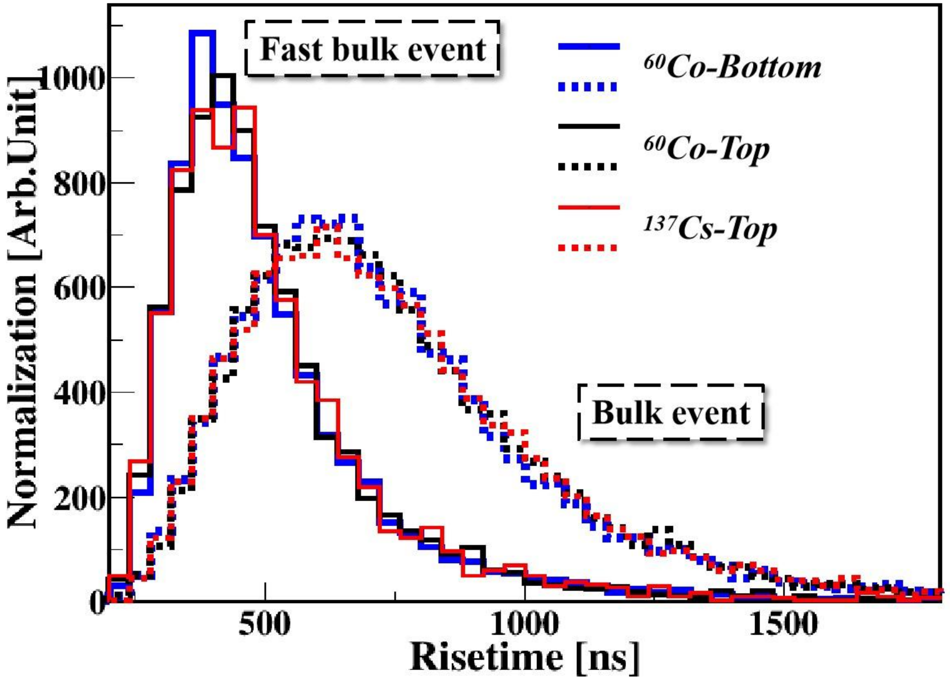

Fig.21 Comparison of the rise-time distributions **at 2–3 keVee** for different source types and different mounting positions (Normalization)

Source type: $^{60}Co/^{137}Cs$

Source position: Top/Bottom

The universality of distribution:

due to the poor spatial resolution in the **low-energy regions** caused by noise, the rise-time distributions of both two types events are almost independent on the source type and position.

It's beneficial for identifying FBEs and BEs in background

BE and FBE discrimination

Ultimate aim: The discrimination of FBEs and BEs in the background

- Various unknown and complex sources: how to determine the PDFs of BEs and FBEs from different type and position of sources?
- Analysis of background (preliminary work)
- Event discrimination below 1keVee?

The universality of distribution:

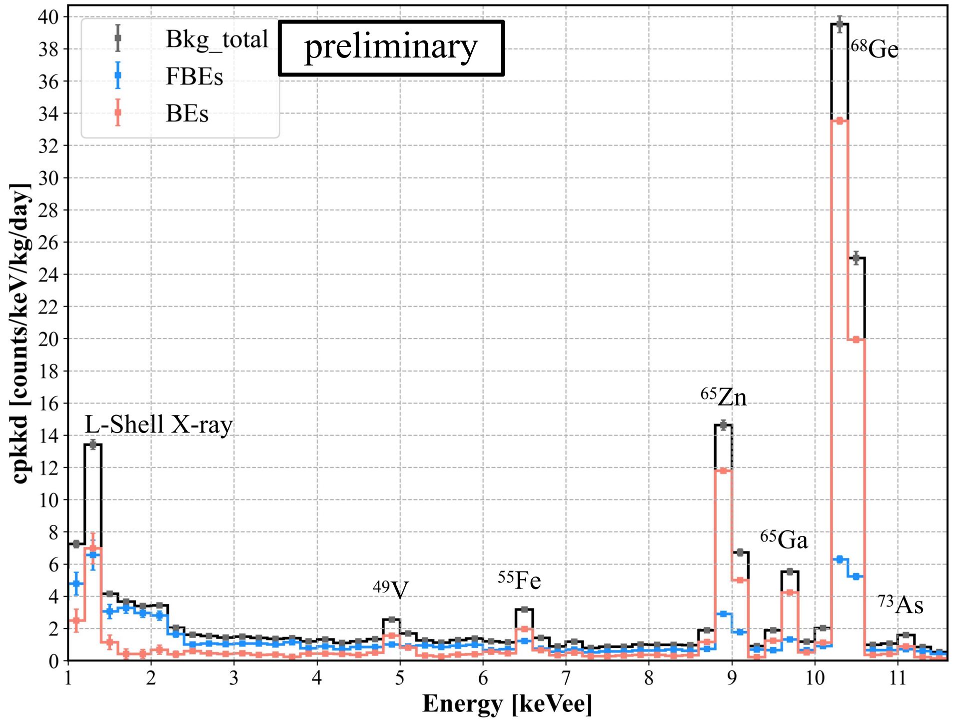

Fig.22 CDEX background spectra in the low energy region, including FBEs and BEs

Characteristics:

① FBE spectrum exhibits a significant increase below 2 keVee, while BE spectrum tends to flatten

② Removing FBEs can significantly reduce the CDEX backgorund

BE and FBE discrimination

Ultimate aim: The discrimination of FBEs and BEs in the background

- Various unknown and complex sources: how to determine the PDFs of BEs and FBEs from different type and position of sources?
- Analysis of background (preliminary work)
- Event discrimination below 1keVee?

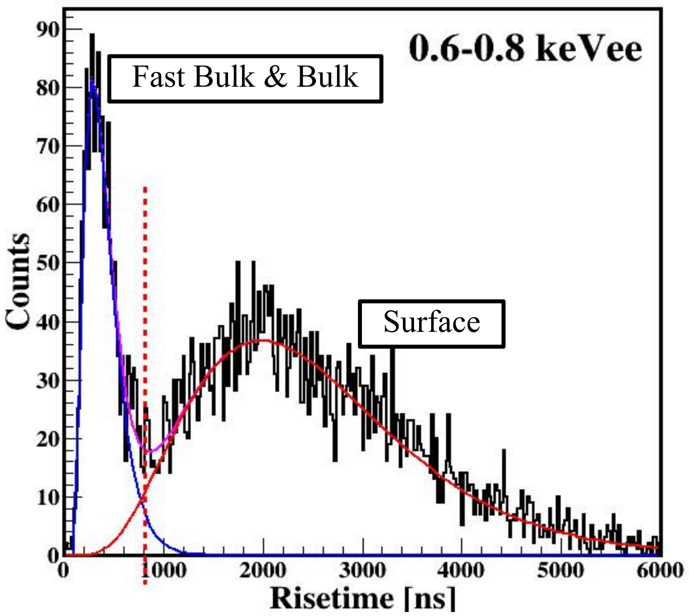

Fig.23 Serious SEs penetration below 1 keVee

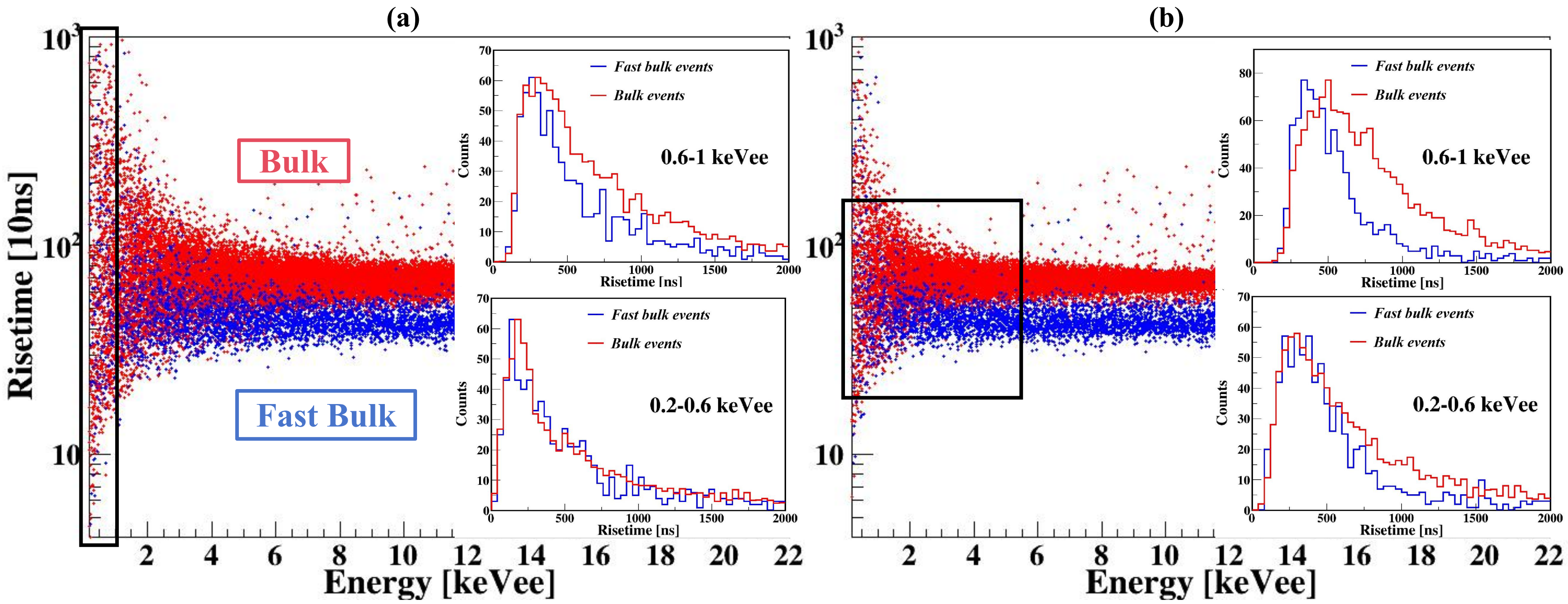

Fig.24 Simulated rise-time distributions of FBEs (blue) and BEs (red) below 1 keVee: **(a)** current noise level; **(b) assuming noise is reduced by half.**

① Serious **SEs penetration** below 1 keVee

② Subtle and insignificant differences between two types events due to electrical noise

③ Reducing electrical noise is expected to further improve the discrimination of FBEs and BEs at low energies.

Summary and prospects

① A thorough study was conducted to better understand the pulse formation, characteristics, and location distribution of FBEs using a semiconductor electric field and pulse shape simulation.

② This study demonstrates an important property of *p*PCGe: single-hit bulk spatial resolution.

③ We provide a method of discriminating between FBEs and BEs. They serve as a basis for better identification of FBEs as background in rare-event searches with germanium detectors.

TAUP XICHANG

THANKS

Li Renmingjie

Sichuan University

CDEX CJPL

PS

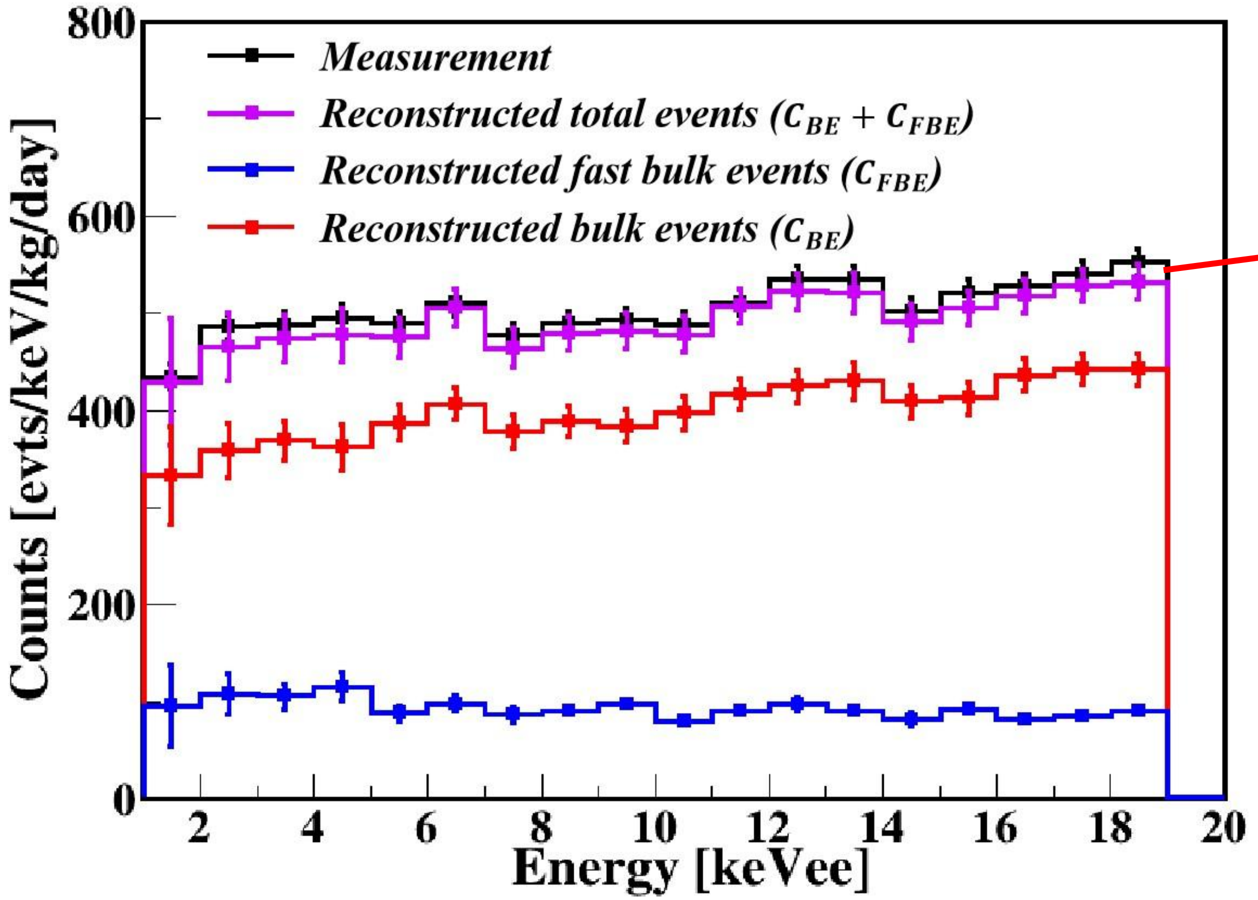

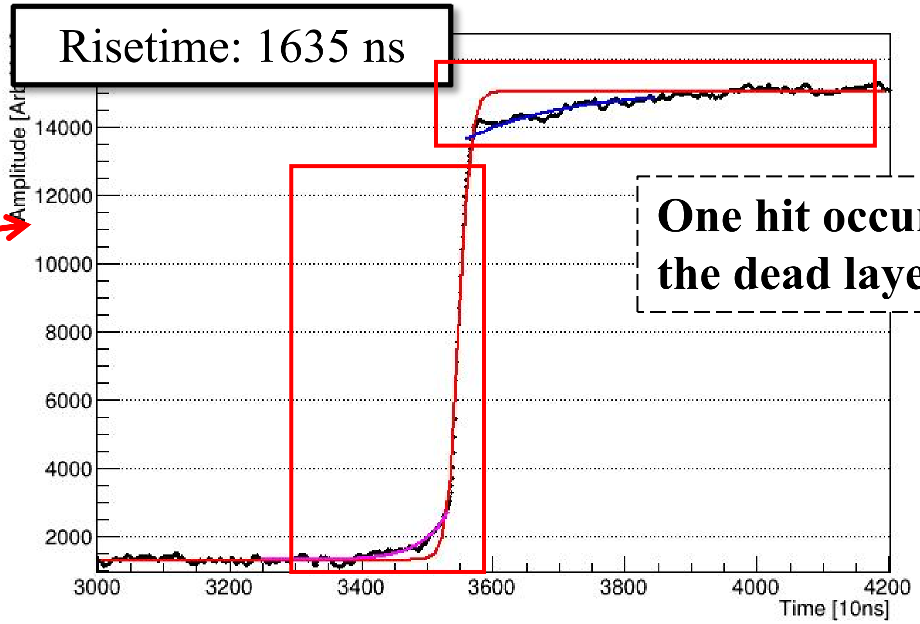

One hit occurs in the dead layer

the other occurs in the bulk/fast region

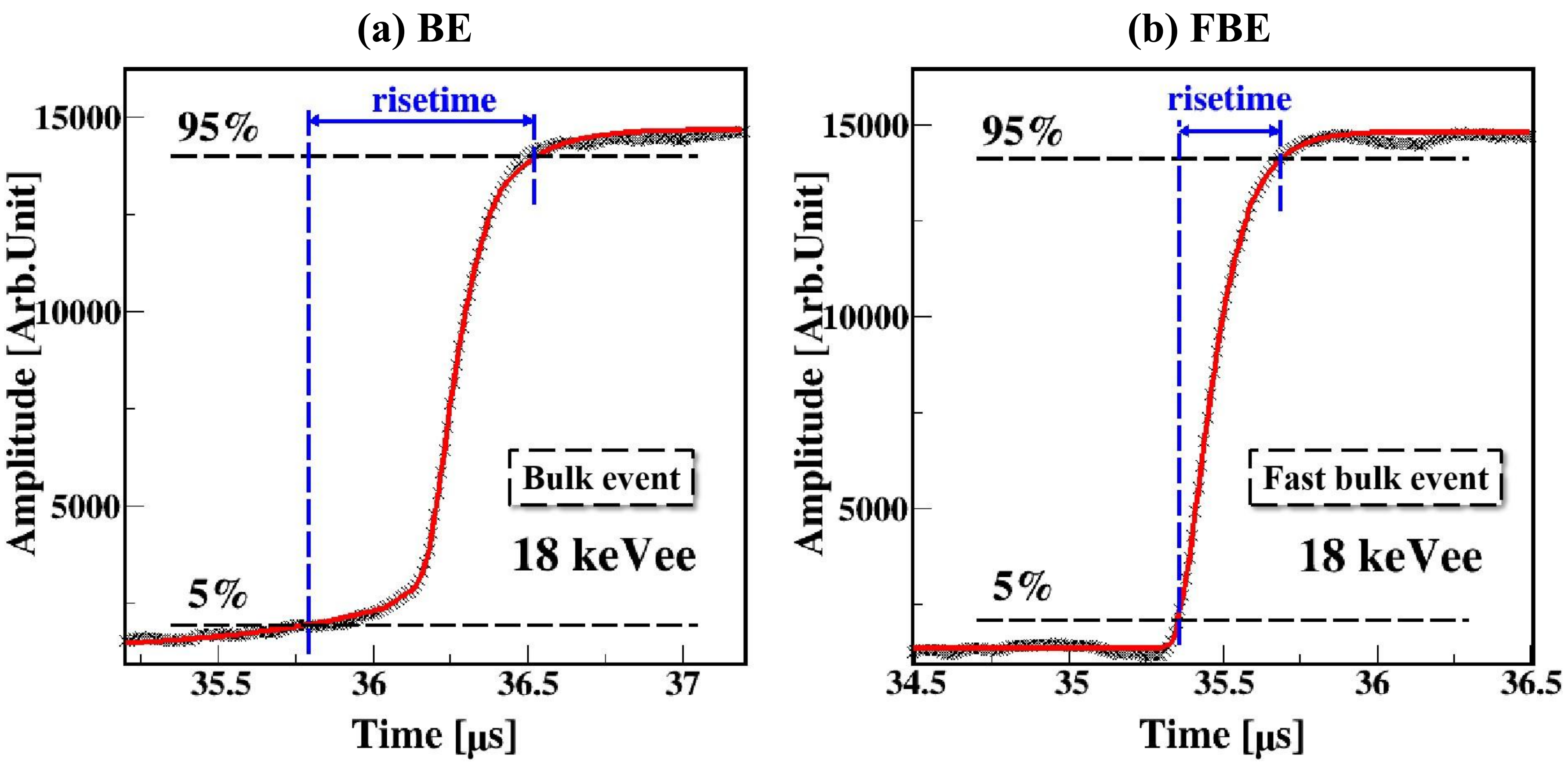

Fig.12 Pulse shape of (a) BE and (b) FBE.

►To accurately describe the pulse shape and reduce the noise effect, the pulse is fitted by two hyperbolic tangent functions at the front and back edges, because of the asymmetry of the pulse shape.

The rise time τ is parameterized by the time interval between 5 and 95% of the amplitude of the fitted function